Distributed Online Monitoring Method and Application of Cable Partial Discharge Based on φ-OTDR

WENXIA PAN[1], KUN ZHAO [ID][1], CHEN XIE[1], XINRUI LI[1], JIE CHEN[2], AND LIBIN HU[2]

[1]College of Energy and Electrical Engineering, Hohai University, Nanjing 210098, China
[2]State Grid Jiangsu Electric Power Company Ltd., Research Institute, Nanjing 211103, China

Corresponding author: Kun Zhao (zhaokun571@163.com)

ABSTRACT Partial discharge (PD) is an early manifestation of multiple cable faults. The traditional PD monitoring method has a weak monitoring effect and low positioning accuracy when monitoring the PD of cable. This paper proposes a distributed on-line monitoring method for cable PD based on phase-sensitive fiber-optic time domain reflection (φ-OTDR) principle. Firstly, the production and propagation model of the partial discharge ultrasonic wave (PDUW) of the cable was established and simulated, and the distribution of PDUW inside the cable with different conditions and different structures was obtained. Then we established a model of cable PDUW, and the backscattered Rayleigh light intensity in fiber and theoretically analyzed and experimentally verified the relationship between the cable PDUW and backscattered Rayleigh light intensity in fiber. The experimental results are consistent with the theoretical analysis. When the cable has PD, the backscattered Rayleigh light intensity change of the PD position is higher than the intact position. We analyzed the experimental data and obtained the judgment conditions of the cable PD. Finally, we calculate and obtain the sensitivity of the monitoring method to different cables and the warning value when cable PD is abnormal.

INDEX TERMS Partial discharges, cable insulation, optical fiber testing, ultrasonic variables measurement, φ-OTDR.

I. INTRODUCTION

Defects in the production and installation of power cables and stresses by electrical, thermal, and mechanical during operation can cause cable insulation to crack and partial discharge (PD) [1]–[3]. PD can cause insulation to crack quickly and cause cable failure at the end, which affects production and even endangers life. Therefore, it is essential to find the partial discharge of the cable as soon as possible to reduce the occurrence of cable faults, improve the reliability of power supply, and ensure the safe and stable operation of the power system.

Electric pulse, electromagnetic wave, luminescence, heat generation, ultrasonic wave, gas generation, and other phenomena occur when cable occurs PD [4], [5]. PD monitoring method mainly judges and locates PD by monitoring the above phenomenon. High-frequency pulse current

monitoring is highly sensitive, but it is susceptible to electro-magnetic interference, and the method has poor positioning accuracy [6], [7]. When the high frequency pulse current method monitors a PD of a short distance cable line, only a high frequency current sensor is required. Long-distance cross-connected cable lines require a large number of sensors and require a dedicated communication network to transmit large amounts of monitoring data [8]. When the cable is cross-connected, the pulse current interferes, which causes a positioning error [9]. The transient earth voltage monitoring method applies to the monitoring of cable terminal joints, branch boxes, switch cabinets, etc., and is not suitable for distributed monitoring of cables [10]. The ultra-high frequency (UHF) method has the advantages of strong anti-interference ability and high sensitivity and has full application in GIS power transformers and cable connectors [11]. When a PD occurs inside the cable, the UHF signal can be transmitted from the cable connector and the ground line to the air. Therefore, the UHF method has poor positioning accuracy for

---

The associate editor coordinating the review of this manuscript and approving it for publication was Boxue Du [ID].

the partial discharge fault inside the cable and UHF signals are attenuated severely over long distances in the air [12]. The ultrasonic monitoring method has the same advantages as UHF [13], [14]. The traditional ultrasonic detection method uses ultrasonic sensors to monitor. When passing through a long-distance and multiple shielding structure, the ultrasonic waves are rapidly attenuated and cannot be detected. Traditional ultrasonic PD detection methods cannot monitor PD of cables in a distributed manner. Distributed optical fiber vibration monitoring technology based on phase-sensitive optical time-domain reflectometry (φ-OTDR) principle can monitor and locate vibration along optical fiber [15], [16]. The partial discharge ultrasonic wave (PDUW) of cables causes the vibration of the surrounding media, so we can monitor the vibration of the PDUW of the cable by distributed fiber vibration monitoring technology and then judge and locate the PD inside the cable [17].

In this paper, we propose an online monitoring method for the PD of cables based on the principle of φ-OTDR. This method uses optical fiber that is pre-positioned inside cables or laid on the surface of cables to monitor the PDUW of cables, and then determine and locate the partial discharge PD of cables. Firstly, we establish and simulate the production and study the distribution of PDUW inside cables with different conditions and different structures. Then, we theoretically analyze and experimentally verify the relationship between the PDUW of the cable and the variation of the backscattered Rayleigh light intensity (BRLI) in the optical fiber. Further, we analyze the experimental data and obtain the judgment conditions of the cable PD. Finally, we calculate and obtain the sensitivity of the monitoring method to different cables and the warning value when cable PD is abnormal.

II. THE PRINCIPLE OF THE ONLINE MONITORING METHOD

In this paper, a model for the generation of PDUW was established, and the calculation method of ultrasonic sound pressure at the PD point was obtained. Then the propagation of the ultrasonic wave inside the cable and the relationship between the ultrasonic sound pressure and the fiber strain were studied. Finally, the relationship between fiber strain and BRLI was analyzed by using the φ-OTDR based acoustic wave monitoring model. Through the above research, we obtained the relationship between the partial discharge of the cable and the change of BRLI in the fiber.

A. GENERATION MODEL OF PDUW

When an air gap occurs in the XLPE cable insulation medium, partial discharge is likely to occur inside the air gap accompanied by ultrasonic generation. The main reason for the generation of ultrasonic waves is that when a PD occurs inside the air gap, the heat of the PD point causes the air pressure of the air gap to increase, and after the PD ends, the heat loss causes the gas pressure to decrease. Repeated PD causes repeated changes in the pressure of the air gap, eventually producing ultrasonic waves.

PD pulse duration is short, about 1-100ns [18]. The PD pulse duration is short, about 1-100 ns, so the heat generated by the PD is concentrated at the PD point, causing the pressure of the small-range air gap ball to increase. The increase in pressure ΔP can be expressed as Eq. (1).

$$\Delta P = P_0 \beta_0 \Delta t \tag{1}$$

where P_0 represents the pressure of the air gap ball at $0°C$, $P_0 = 101325Pa$. β_0 represents the coefficient of expansion of the air gap ball at $0°C$, $\beta_0 = 3.66 \times 10^{-3} K^{-1}$. Δt is the temperature change of the air gap. Its expression is Eq. (2).

$$\Delta t = \lambda W / C_v m \tag{2}$$

In Eq. (2), W is the energy of single PD. $W = \Delta q U / 2$, Δq apparent discharge magnitude. U is cable operating voltage. λ is the percentage of thermal expansion energy in the total energy of PD, and its value range is 0.03-0.08 [19]. C_v is the specific heat at constant volume of the air gap ball under normal working temperature and pressure, m is the mass of the air gap ball. $m = 4\pi R^3 \rho / 3$. R is the radius of the air gap ball, $R = 0.2mm \sim 0.6mm$ [20]. ρ is the density of the air gap ball.

Bringing the Eq. (2) into the Eq. (1), the increase in air gap ball pressure ΔP when the cable occurs PD, and the pressure of the PDUW p_R can be obtained.

$$p_R = \Delta P = \frac{3P_0 \beta_0 \lambda \Delta q U}{8 C_v \pi R^3 \rho} \tag{3}$$

Eq. (3) is the equation of discharge and the PDUW pressure, and when the discharge of the cable is known, the PDUW pressure of the PD point can be calculated. It can be known from Eq. (3) that the more considerable discharge, the higher the PDUW pressure at the PD point.

B. ANALYSIS OF PDUW PROPAGATION AND FIBER DEFORMATION

Cables are made up of a variety of materials to form a complex structure. The PDUW generated at the PD point is transferred to the surface of the cable through a complicated process. This paper only considers the shortest path from the PD point to the cable surface, which is perpendicular to the interface of the cable insulation medium. The PDUW of the cable belongs to the spherical wave and belongs to the longitudinal wave because the vibration direction of the wave is the same as the propagation direction [21]. Due to inertia, the air gap ball will vibrate continuously and damply, and repeated PD generates continuous PDUW.

A schematic diagram of the spherical wave propagating in a n-layer media is shown in Figure 1. In Figure 1a, p_s is a sound source. M_i and M_{i+1} is the intermediate medium with limited thickness, representing the intermediate medium on the PDUW propagation path inside the cable. M_n is the infinite outer medium, representing the environmental medium (air or soil) outside the cable. Figure 1b is the equivalent calculation model of reflection in Figure 1a.
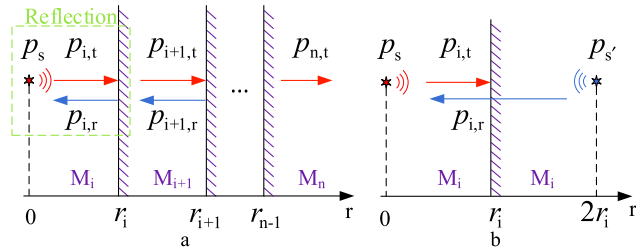
FIGURE 1. a. Schematic diagram of spherical wave propagation in *n*-layer media, b. Equivalent calculation model of reflection.

According to acoustic theory in [22], [23], when the time is *t*, the complex expressions of the spherical wave pressure $p_{M_i}(t, r)$ and the particle vibration velocity $v_{M_i}(t, r)$ at the point in medium M_i with distance *r* from sound source are expressed as Eq. (4) and Eq. (5).

$$p_{M_i}(t, r) = \frac{A_i}{r} e^{-\alpha_i r} e^{j(\omega t - kr)}$$
$$+ \frac{B_i}{2r_i - r} e^{-\alpha_i(2r_i - r)} e^{j(\omega t - k(2r_i - r))} \quad (4)$$

$$v_{M_i}(t, r) = \frac{A_i}{r \rho c}\left(1 + \frac{1 + \alpha_i r}{jkr}\right) e^{-\alpha_i r} e^{j(\omega t - kr)}$$
$$- \frac{B_i}{\rho c (2r_i - r)}\left(1 + \frac{1 + \alpha_i (2r_i - r)}{jk (2r_i - r)}\right)$$
$$\times e^{-\alpha_i(2r_i - r)} e^{j(\omega t - k(2r_i - r))} \quad (5)$$

where A_i is the amplitude of $p_{i,t}$ at $1m$ from the sound source p_s in Figure 1b, and $p_{i,t}$ is the sound pressure of the incident or refracted wave in M_i. B_i is the amplitude of $p_{i,r}$ at $1m$ from the sound source $p_{s'}$ in Figure 1b, and $p_{i,r}$ is the sound pressure of the reflected wave in M_i. $p_{s'}$ is a virtual sound source, and is symmetric with the p_s. The symmetry plane is the interface between M_i and M_{i+1}. M_i and M_{i+1} are two different media. When the outermost medium is infinite, the reflected wave B_i is 0. $\alpha_i = \omega\eta/(2c_a)$, η is the loss coefficient of the medium M_i, metal is 0.001, and composite is 0.1. $\omega = 2\pi f_a$, f_a is sound wave frequency. $k = \omega/c_a$, c_a is sound wave speed. r_i is the distance between the media interface of M_i and M_{i+1} from the sound source.

Sound pressure and particle vibration velocity are continuous at the interface. The boundary condition at the interface is Eq. (6).

$$\begin{cases} p_{M_i}(t, r_i) = p_{M_{i+1}}(t, r_i) \\ v_{M_i}(t, r_i) = v_{M_{i+1}}(t, r_i) \end{cases} \quad (6)$$

Bringing the Eq. (4) and Eq. (5) into the Eq. (6), the matrix propagation equation (7) of the two-layer medium can be obtained.

$$T_{r_i, i+1}\begin{bmatrix} A_{i+1} \\ B_{i+1} \end{bmatrix} = T_{r_i, i}\begin{bmatrix} A_i \\ B_i \end{bmatrix} \quad (7)$$

where $T_{r_i, i}$, $T_{r_i, i+1}$ are the propagation matrices of the medium M_i and M_{i+1}, respectively. The matrix is a constant matrix when mediums are known.
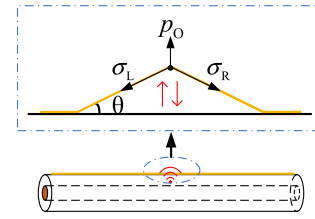

FIGURE 2. Schematic diagram of sensing fiber deformation.

Through the recursive relationship of Eq. (7), we can get the propagation Eq. (8) of the PDUW from the cable PD point to the external environment.

$$\begin{bmatrix} A_n \\ B_n \end{bmatrix} = T_{r_n, n+1}^{-1} T_{r_n, n} \cdots T_{r_i, i+1}^{-1} T_{r_i, i}\begin{bmatrix} A_1 \\ B_1 \end{bmatrix} \quad (8)$$

A_n and B_n are the variables of the outermost medium. The outermost layer is air or soil, approximately infinite medium, $B_n = 0$. The relationship between A_1 and P_R is $p_R = A_1/R$ [24].

Solving Eq. (8), we can obtain A_n and B_1, and bring them into Eq. (7) to get A_i and B_i for each layered medium. Finally, bringing A_i and B_i into Eq. (4), we can get the sound pressure at each point on the propagation path, including the sound pressure p_o of the PDUW of the cable at the sensing fiber.

After the above analysis, the sound pressure p_o can be obtained, and then the influence of the PDUW on the deformation of the sensing fiber can be studied.

C. ACOUSTIC WAVE MONITORING MODEL BASED ON ϕ-OTDR

When the PDUW of the cable propagates to the sensing fiber, the acoustic vibration causes the sensing fiber to deform. The deformation of the sensing fiber is shown in Figure 2.

According to Figure 2, we can establish the equation of the relationship between fiber strain $\Delta\varepsilon$ and sound pressure and solve the equation to obtain the fiber strain change $\Delta\varepsilon$.

$$\begin{cases} E\Delta\varepsilon \sin\theta = p_O \\ \dfrac{1}{1 + \frac{\Delta\varepsilon}{2}} = \cos\theta \end{cases} \quad (9)$$

where p_O is the PDUW pressure at the sensing fiber. E is Young's modulus of the fiber, $E = 7 \times 10^{10}$Pa. Eq. (9) shows that the higher the sound pressure, the greater the amount of fiber strain change.

Because the BRLI in the fiber changes after the deformation of the sensing fiber, we can monitor the PDUW by monitoring the change of the BRLI to determine and locate the PD of the cable.

A schematic diagram of a one-dimensional impulse response model of BRLI is shown in Figure 3.

The expression of BSRLI in [25] is Eq. (10), Eq. (11) and Eq. (12).

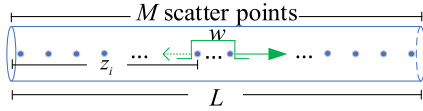$$I_k(t) = |e(t)|^2 = I_k'(t) + I_k''(t) \quad (10)$$

FIGURE 3. Schematic diagram of the one-dimensional impulse response model for BRLI.

$$I_k'(t) = \sum_{i=1}^{N} a_i^2 e^{\left(-2\alpha \frac{c\tau_i}{n_f}\right)} rect\left(\frac{t-\tau_i}{W}\right) \quad (11)$$

$$I_k''(t) = 2\sum_{i=1}^{N}\sum_{j=i+1}^{N}\left(\begin{matrix} a_i a_j \cos\left(\varphi_{ij}+\Delta\varphi_{ij}\right) e^{\left(-\alpha \frac{c(\tau_i+\tau_j)}{n_f}\right)} \\ \times rect\left(\frac{t-\tau_i}{W}\right) rect\left(\frac{t-\tau_j}{W}\right)\end{matrix}\right) \quad (12)$$

where k represents the k_{th} measurement, and N is the number of scattering centers in the fiber. a_i is the scattering coefficient of the i_{th} scattering center. α is the fiber attenuation coefficient. c is the speed of light in vacuum. n_f is the refractive index of the fiber. τ_i is the delay time of the scattered light at the i_{th} scattering center, $\tau_i = 2n_f z_i / c$ and z_i is the position of the scattering center. W is the width of the light pulse. $rect\left((t-\tau_i)/W\right)$ is a rectangular function, $0 \le (t-\tau_i)/W \le 1$, $rect\left((t-\tau_i)/W\right) = 1$, otherwise is 0. φ_{ij} is the optical phase difference between the scattering center i and j. $\Delta\varphi_{ij}$ is the amount of change in φ_{ij} caused by fiber deformation and the expression of $\Delta\varphi_{ij}$ is Eq. (13).

$$\Delta\varphi_{ij} = \frac{4\pi}{\lambda}\left(n_f + C_\varepsilon\right) z_{ij}\Delta\varepsilon \quad (13)$$

where λ is the wavelength of light. C_ε is the strain coefficient of the refractive index [26]. Because the pressure of the sound wave is small, the strain change of the fiber is small and $\Delta\varphi_{ij} \ll \pi/2$.

The BRLI change of each scattering center in the fiber, $\Delta I_k(z_i)$, is Eq. (14).

$$\Delta I_k(z_i) = I_k(z_i) - I_{k-1}(z_i) \quad (14)$$

where $z_i = tc/2n_f$.

It can be seen from the above analysis that the larger the PD of the cable, the stronger the PDUW of the cable, and the greater the strain variation of the optical fiber. When $\Delta\varphi_{ij} \ll \pi/2$, it can be known from Eq. (13) and Eq. (15) that the larger the strain variation of the fiber, the larger BRLI variation of the fiber.

To determine and locate the PD of the cable, we specify M measurements as one measurement cycle. The vibration magnitude of each scattering center in a measurement cycle is determined by the vibration coefficient K_i. The expression of K_i is as Eq. (15).

$$\frac{\sum_{k=1}^{M} \Delta I_k(z_i)}{\sum_{k=1}^{M} \Delta I_k(z_{st})} = K_i \quad (15)$$

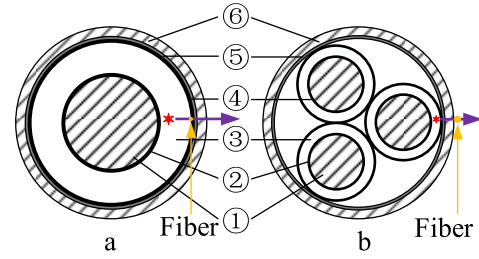where z_{st} is the reference segment which is no PD.

FIGURE 4. Cable cross-section diagram.

TABLE 1. Cable structural parameters.

Structural	a	b	$\rho\left(kg/m^3\right)$	$c_a\left(m/s\right)$
①cored wire	30.3	23.8	8940	5240
②Conductor shield	1.2	0.8	930	1900
③XLPE Insulation	20.1	4.6	930	1900
④Insulating shield	1	0.8	930	1900
⑤Aluminum sheath	2	0.8	2770	6250
⑥Outer sheath	4.5	4	1330	2388

The Eq. (15) shows that the higher vibration coefficient is at a certain point, the more enormous change in the BRLI is, and the more considerable discharge is.

The discharge of the cable is too small to cause the fiber to vibrate. At this time, the method cannot detect the PD of the cable. Therefore, this method has a limit on the minimum measurable amount of PD. The minimum measurable discharge is defined as the sensitivity of the monitoring method, and the vibration coefficient of the sensitivity is determined as the vibration threshold K_{th}. When $K_i \ge K_{th}$, there is a PD fault at the corresponding position of the cable.

III. SIMULATION AND EXPERIMENT

In this paper, we establish a PDUW generation model of cable, analyze the distribution of PDUW inside the cable and the influence of PDUW on the deformation of the fiber and study the relationship between the strain of the fiber and the change of the BRLI in the fiber. Finally, we obtain the method of judging and locating the PD of the cable by the change of the BRLI in the fiber. We set up experiments to verify the feasibility of the method.

There are two ways to install fiber: presetting inside the cable and laying on the cable surface. This article chose two types of cables for simulation: YJLW03-1×630-64/110kV and YJV-3×400-8.7/10kV. The cable cross-section diagram is shown in Figure 4, and the structure parameters are in Table 1.

According to the actual working condition of the cable, for calculation and simulation, the voltage to ground of the 110kV cable is set to 63.5kV and 10kV cable is 7kV. The average of apparent charge of PD is 100pC. The 110kV cable PD point is located at 4.85 *mm* from the surface of the core wire, and 10kV is 1.75 *mm*. The position of the sensing fiber is shown in Figure 4.
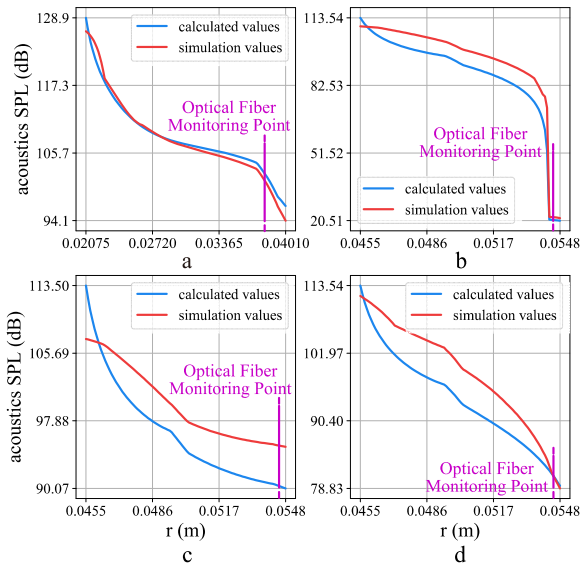
FIGURE 5. Comparison of calculation and simulation results of PDUW distribution in the cable; a. PDUW distribution of 110kV cable, b. PDUW distribution of a 10kV cable in a tunnel when the sensing fiber and cable are not tightly attached, c. PDUW distribution of buried 10kV cable, d. PDUW distribution of a 10kV cable in a tunnel when the sensing fiber and cable are tightly attached.

A. CALCULATION AND SIMULATION COMPARISON OF PDUW DISTRIBUTION IN THE CABLE

According to the actual working condition of the cable, for calculation and simulation, the voltage to ground of the 110kV cable is set to 63.5kV and 10kV cable is 7kV. The average of apparent charge of PD is 100pC. The 110kV cable PD point is located at 4.85 *mm* from the surface of the core wire, and 10kV is 1.75 *mm*. The position of the sensing fiber is shown in Figure 3. The internal average temperature of the cable is 45°C, and the air pressure is 1 atm. The radius of the cable air gap is set to 0.5 *mm*, and density is $\rho = 1.1037\text{k}g/\text{m}^3$.

By calculating Eq. (3) and Eq. (4), the 110kV cable A_1 is 0.04252Pa·m and the 10kV cable is 0.00441Pa·m. The comparison between the sound pressure calculation results on the path shown in Figure 4 and the Ansys simulation results are shown in Figure 5.

In Figure 5, the maximum error between the calculation result and the simulation result is 4.8% in Figure 5c. The model of cable PDUW can accurately calculate the distribution of PDUW. The pre-set and the surface fiber of buried cable can monitor stranger sound pressure, so the PD monitoring is better. In the tunnel, when the surface fiber is tightly attached to the cable, the monitored sound pressure is much higher than when the fit is not tight. Therefore, when monitoring the PD of the cable in the tunnel, the fiber and cable surface needs to be tightly fitted.

B. CALCULATION AND EXPERIMENT OF OPTICAL FIBER MEASURING PD

The type of cables used in the experiment was YJV -3×400-8.7/10kV. Optical fiber sensing equipment was φ-OTDR fiber
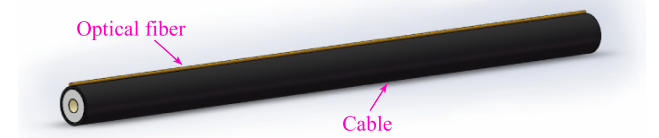

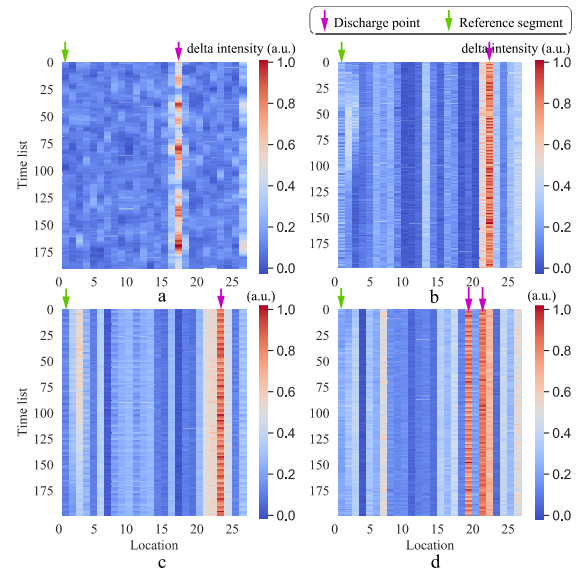FIGURE 6. The arrangement of the fiber out the cables.

FIGURE 7. The BRLI change results of simulation and experiment; a. Simulation and calculation, b. Scratch experiment, c. Micropores experiment, d. Suspended electrode experiment with 2 PD points. The simulation calculation model is that the fiber and cable are tightly attached in a tunnel. The PDUW pressure at the fiber monitoring point is 81.886dB, and the frequency of PDUW is 38kHz [27].

vibration monitor. The experiment was carried out on the cable PD experimental monitoring platform. Figure 6 shows the arrangement of the fiber out the cables.

There are three types of PD faults: scratches, micropore, and floating electrodes in the cable. During the experiment, the voltage applied to the cable was 7kV, and the average discharge of the scratch and the suspended electrode are about 100pC, and the micropore is 200pC. The simulation calculation was 100pC. The sensing fiber is single-mode fiber with a length of 60 *m*. The fiber is laid tightly on the cable surface. Reference segment at the head of the cable.

Figure 7 is the BRLI change results of simulation and experiment.

In Figure 7, color indicates the degree of BRLI change in the fiber. The redder the color is, the more the degree of BRLI change is. In Figure 7a, we set up the PD point at location 17 and the reference point at location 1. The color at location 17 is redder than location 1. In Figure 7b, 7c and 7d, we test the PD of cables. The results show that PD points color is redder than reference segments. The conclusion of the theoretical analysis is consistent with the experimental results. The degree of BRLI change at the PD points is significantly greater than the intact position. Using the heat

TABLE 2. The vibration coefficient of simulation calculation and experimental results.

Simulation and experiment / Vibration coefficient	K_i
Reference segment (0pC)	1
Simulation (100pC)	3.68
Scratch (100pC)	3.46
Micropores (200pC)	6.07
Suspended electrode PD1 (100pC)	3.48
Suspended electrode PD2 (100pC)	3.63

TABLE 3. The sensitivities of different cables.

Cable	Sensitivity (pC)
110kV cable with preset fiber	8
10kV buried cable	18
10kV tunnel cable	50

map like Figure 7, we can visually find and locate the PD of the cable. Figure 7d contains two PD points. The results show that the method can monitor and locate multiple PD faults on the cable.

In Table 2, the vibration coefficient of simulation is approximately equal to the vibration coefficient of the experiment of the equivalent discharge. The main cause of the error is the constant change of the discharge during the experiment. However, we use the average value in the simulation. Also, when the partial discharge amount increases, the vibration coefficient increases, which is consistent with the theoretical analysis result of Eq. (16). Therefore, we can use the vibration coefficient to estimate the severity of the cable PD.

When the discharge is higher than 300pC, the cable is in an abnormal state [28]. At this time, the theoretical calculation value of the vibration coefficient of the experimental cable in this paper is $K = 11.97$. Therefore, for the same type of cable, when $K \geq 11.97$, the cable status is abnormal and should be monitored.

It can be seen from Eq. (16) that when $K_{th} = 3$, the method can clearly distinguish the PD of the cable, and the sensitivities of the 110kV cable (YJLW03-1×630-64/110kV) and 10kV cable (YJV-3×400-8.7/10kV) in this paper can be obtained by theoretical calculation and are shown in Table 3.

Table 3 shows that the monitoring method in this paper has different sensitivities for different cables. Cable with preset fiber and buried cable are more sensitive than without preset fiber cable in a tunnel.

IV. CONCLUSION

In this paper, we propose an online monitoring method for PD of cables based on the principle of φ-OTDR and verify the feasibility of this method through simulation, calculation, and experiment. Analyzing the research results, we get the following conclusions.

1) The monitoring method in this paper can better monitor the cable with preset fiber and the buried cable. In order to better monitor the cable without pre-set fiber in the tunnel, the fiber and cable surface need to be tightly fitted.
2) The monitoring method in this paper has different sensitivities for different cables. Cable with preset fiber and buried cable are more sensitive than without preset fiber cable in a tunnel.
3) The cable PD monitoring method proposed in this paper can detect and locate the cable PD in time and alarm the abnormal state. It is of considerable significance to reduce significant cable faults, extend the service life of the cable, and ensure the safe and stable operation of the cable.

REFERENCES

[1] N. Ra, N. S. B. Mustafa, T. Kawashima, Y. Murakami, and N. Hozumi, "Development of a partial discharge measuring method for a long-distance cable line," *IEEJ Trans. Elect. Electron. Eng.*, vol. 14, no. 7, pp. 996–1001, Jul. 2019.

[2] J. Granado, A. Torralba, and C. Álvarez-Arroyo, "Partial discharge detection using PLC receivers in MV cables: A theoretical framework," *Electr. Power Syst. Res.*, vol. 164, pp. 61–69, Nov. 2018.

[3] A. Hekmati and R. Hekmati, "Optimum acoustic sensor placement for partial discharge allocation in transformers," *IET Sci. Meas. Technol.*, vol. 11, no. 5, pp. 581–589, 2017.

[4] A. R. Mor, L. C. C. Herdia, and F. A. Muñoz, "A novel approach for partial discharge measurements on GIS using HFCT sensors," *Sensors*, vol. 18, no. 12, p. 4482, Dec. 2018.

[5] D. Dukanac, "Application of UHF method for partial discharge source location in power transformers," *IEEE Trans. Dielectr. Elect. Insul.*, vol. 25, no. 6, pp. 2266–2278, Dec. 2018.

[6] B. Sheng, C. Zhou, D. M. Hepburn, X. Dong, G. Peers, W. Zhou, and Z. Tang, "Partial discharge pulse propagation in power cable and partial discharge monitoring system," *IEEE Trans. Dielectr. Elect. Insul.*, vol. 21, no. 3, pp. 948–956, Jun. 2014.

[7] W. Pan, M. Liu, K. Zhao, Y. Zhang, and T. Liu, "A practical short-circuit current calculation method for DFIG-based wind farm considering voltage distribution," *IEEE Access*, vol. 7, pp. 31774–31781, 2019.

[8] L. Zhang, B. Sheng, W. Jiang, W. Zhou, Z. Tian, X. Dong, and Z. Tang, "On-line PD detection and localization in cross-bonded HV cable systems," *High Voltage Eng.*, vol. 41, no. 8, pp. 2706–2715, Aug. 2015.

[9] W. Wang, Y. Wang, C. Liu, Y. Li, D. Zhang, Y. Sun, and W. Wang, "Partial discharge simulation analysis and frequency-dependent model for 110 kV three-phase cross-bonded cable," *Proc CSEE*, vol. 31, no. 1, pp. 117–122, Jun. 2011.

[10] C. Zhang, M. Dong, M. Ren, W. Huang, J. Zhou, X. Gao, and R. Albarracín, "Partial discharge monitoring on metal-enclosed switchgear with distributed non-contact sensors," *Sensors*, vol. 18, no. 2, p. 551, Feb. 2018.

[11] A. Darwish, S. S. Refaat, H. A. Toliyat, and H. Abu-Rub, "On the electromagnetic wave behavior due to partial discharge in gas insulated switchgears: State-of-art review," *IEEE Access*, vol. 7, pp. 75822–75836, 2019.

[12] J. Pu, "Development of an on-line partial discharge detection system for power cables," M.S. thesis, Dept. Elect. Eng., Harbin Univ. Sci. Technol., Univ., Harbin., Heilongjiang, China, 2013.

[13] G.-M. Ma, H.-Y. Zhou, C. Shi, Y.-B. Li, Q. Zhang, C.-R. Li, and Q. Zheng, "Distributed partial discharge detection in a power transformer based on phase-shifted FBG," *IEEE Sensors J.*, vol. 18, no. 7, pp. 2788–2795, Apr. 2018.

[14] W. Qi, J. Li, B. Chen, J. Yuan, and Y. Zhong, "Ultrasonic wave propagation characteristics of the transformer based on COMSOL," *Trans. China Electrotech. Soc.*, vol. 30, sup. 2, pp. 195–200, 2015.

[15] Y. Lu, T. Zhu, L. Chen, and Y. Bao, "Distributed vibration sensor based on coherent detection of phase-OTDR," *J. Lightw. Technol.*, vol. 28, no. 22, pp. 3243–3249, Nov. 15, 2010.

[16] M. Liu, W. Pan, Y. Zhang, K. Zhao, S. Zhang, and T. Liu, "A dynamic equivalent model for DFIG-based wind farms," *IEEE Access*, vol. 7, pp. 74931–74940, 2019.

[17] X. Bao, D.-P. Zhou, C. Baker, and L. Chen, "Recent development in the distributed fiber optic acoustic and ultrasonic detection," *J. Lightw. Technol.*, vol. 35, no. 16, pp. 3256–3267, Aug. 15, 2017.

[18] R. Bartnikas and J. P. Novak, "On the spark to pseudoglow and glow transition mechanism and discharge detectability," *IEEE Trans. Elect. Insul.*, vol. 27, no. 1, pp. 3–14, Feb. 1992.

[19] Q. Liu, H. Shao, and Y. Zhang, "Study on shock waves induced by electric spark discharge," *China Sci. Paper*, vol. 11, no. 23, pp. 2649–2653, Dec. 2016.

[20] G. Liu and Z. Chen, "Experiment of main insulation with air gap of 10 kV cross linked polyethylene cable terminal," *High Voltage Eng.*, vol. 38, no. 3, pp. 678–683, Mar. 2012.

[21] T. Jing, "Research on on-line detection method of partial discharge in cable," M.S. thesis, Dept. Elect. Eng., Shenyang Technol. Univ., Shenyang, China, 2017.

[22] D. Ma, "Plane wave propagation," in *Modern Acoustic Theory*, 1st ed. Beijing, China: Science Press, 2004, pp. 65–85.

[23] F. J. Fahy and P. Gardonio, "Waves in fluids and solid structures," in *Sound and Structural Vibration*, 2nd ed. Oxford, U.K.: Academic, 2007, pp. 1–14.

[24] P. M. Morse and K. U. Ingard, "Chapter 7 the radiation of sound," in *Theoretical Acoustics*, 1st ed. New York, NY, USA: McGraw-Hill, 1986, pp. 306–332.

[25] L. Zhou, F. Wang, X. Wang, Y. Pan, Z. Sun, J. Hua, and X. Zhang, "Distributed strain and vibration sensing system based on phase-sensitive OTDR," *IEEE Photon. Technol. Lett.*, vol. 27, no. 17, pp. 1884–1887, Sep. 1, 2015.

[26] J. J. Carr, S. L. Saikkonen, and D. H. Williams, "Refractive index measurements on single-mode fiber as functions of product parameters, tensile stress, and temperature," *Fiber Integr. Opt.*, vol. 9, no. 4, pp. 393–396, Oct. 1990.

[27] B. Wang, "Research on high voltage switchgear partial discharge on-line monitoring based on ultrasonic sensor," M.S. thesis, Dept. Elect. Eng., South China Technol. Univ., Guangzhou, China, 2017.

[28] *Test Code for Power Cables*, STATE Grid Corp. China, Beijing, China, 2015.

WENXIA PAN received the B.S. and M.S. degrees from Wuhan University, Wuhan, China, in 1982 and 1987, respectively, and the Ph.D. degree from Hohai University, Nanjing, China, in 2004, where she is currently a Professor of electrical engineering. She has published two research books and authored or coauthored more than 100 journal articles. Her current research interests include renewable energy generation systems, and high voltage and insulation technology.

KUN ZHAO received the B.S. degree in electrical engineering, in 2017. He is currently pursuing the M.S. degree in electrical engineering with Hohai University, Nanjing, China. His main research interests include wind power generation technology, and high voltage and insulation technology.

CHEN XIE received the B.S. degree in electrical engineering, in 2017. He is currently pursuing the M.S. degree in electrical engineering with Hohai University, Nanjing, China. His main research interests include wind power generation technology, and high voltage and insulation technology.

XINRUI LI received the B.S. degree in electrical engineering, in 2016. She is currently pursuing the M.S. degree in electrical engineering with Hohai University, Nanjing, China. Her main research interests include wind power generation technology, and high voltage and insulation technology.

JIE CHEN was born in Anhui, China. He received the B.S. degree from the Harbin Institute of Technology and the Ph.D. degree from Tsinghua University, China. Since 2012, he has been with State Grid Jiangsu Electric Power Company Ltd., Research Institute, Nanjing, China. He has co-published one research book and authored or coauthored more than 30 articles. His main research interests include high voltage and insulation technology, especially power cable technology and power transmission technology.

LIBIN HU received the B.S. and Ph.D. degrees from Xi'an Jiaotong University, Xi'an, China, in 2009 and 2015, respectively. Since 2015, she has been with State Grid Jiangsu Electric Power Company Ltd., Research Institute, Nanjing, China. She has copublished one research book and authored or coauthored more than ten articles. Her current research interests include high voltage and insulation technology, especially power cable technology.

• • •